View metadata, citation and similar papers at core.ac.uk

brought to you by CORE

provided by Elsevier - Publisher Connector

Cell, Vol. 97, 743–754, June 11, 1999, Copyright ©1999 by Cell Press

Simple, but Not Branched, Plasmodesmata Allow the Nonspecific Trafficking of Proteins in Developing Tobacco Leaves

Karl J. Oparka,*§ Alison G. Roberts,* Petra Boevink,* Simon Santa Cruz,* Ian Roberts,* Katja S. Pradel,* Astrid Imlau,† Guy Kotlizky,‡ Norbert Sauer,† and Bernard Epel‡

*Unit of Cell Biology
Scottish Crop Research Institute
Invergowrie
Dundee DD2 5DA
United Kingdom

†Lehrstuhl Botanik II
Molekulare Pflanzenphysiologie
Universität Erlangen-Nurnberg
D-91058 Erlangen
Germany

‡Department of Plant Sciences
Tel Aviv University
Tel Aviv 69978
Israel

Summary

Leaves undergo a sink–source transition during which a physiological change occurs from carbon import to export. In sink leaves, biolistic bombardment of plasmids encoding GFP-fusion proteins demonstrated that proteins with an M_r up to 50 kDa could move freely through plasmodesmata. During the sink–source transition, the capacity to traffic proteins decreased substantially and was accompanied by a developmental switch from simple to branched forms of plasmodesmata. Inoculation of sink leaves with a movement protein-defective virus showed that virally expressed GFP, but not viral RNA, was capable of trafficking between sink cells during infection. Contrary to dogma that plasmodesmata have a size exclusion limit below 1 kDa, the data demonstrate that nonspecific "macromolecular trafficking" is a general feature of simple plasmodesmata in sink leaves.

Introduction

Plasmodesmata are membranous channels that connect higher plant cells to form a functional intercellular communication network (Goodwin, 1983; Lucas et al., 1993; Kragler et al., 1998). Following the formation of a new cell wall, simple plasmodesmata are formed. These plasmodesmata are primary in origin (i.e., they are laid down at cytokinesis) and comprise a single plasma membrane–lined channel containing an axial ER-derived membrane termed the desmotubule (Hepler, 1982; Overall et al., 1982). During cell elongation, simple plasmodesmata may undergo varying degrees of structural alteration. A common form of modification involves branching of the plasmodesmal channel to produce a complex plasmodesma that contains a conspicuous central cavity (Ding et al., 1992; Ding and Lucas, 1996; Ehlers and Kollmann, 1996; Itaya et al., 1998). In addition, some cells lay down secondary plasmodesmata that are formed entirely de novo across preexisting cell walls (Kollmann and Glockmann, 1985, 1991). At present the functional significance, if any, of these variations in plasmodesmal structure is unknown.

Initial studies of plasmodesmata gave rise to a consensus that only small molecules of less than 1 kDa move freely between plant cells (Tucker, 1982; Goodwin, 1983; Erwee and Goodwin, 1985; Terry and Robards, 1987; Burnell, 1988). However, many systemic plant viruses are known to move through plasmodesmata, with the mechanism of movement varying between viral groups (see reviews by Carrington et al., 1996; Gilbertson and Lucas, 1996). A common feature of viral movement is a substantial increase in the size exclusion limit (SEL) of plasmodesmata, allowing the viral genome to pass between cells (Carrington et al., 1996; Oparka et al., 1997). For several viruses, specific movement proteins (MPs) are thought to play a role in the modification of the plasmodesmal pore (Fenczik et al., 1996; Gilbertson and Lucas, 1996; Oparka et al., 1997). MPs have been shown to target plasmodesmata (Tomenius et al., 1987; Epel et al. 1996; Oparka et al., 1997; Blackman et al., 1998), increase the SEL of the pore (Wolf et al., 1989, 1991), and may also traffic viral RNA between cells (Fujiwara et al., 1993; Waigmann et al., 1994).

Recent investigations suggest that plants possess their own macromolecular trafficking system (Mezitt and Lucas, 1996; Kuhn et al., 1997; Jorgensen et al., 1998; Kragler et al., 1998), facilitating the plasmodesmal movement of endogenous RNA molecules (Lucas et al., 1993; Lucas, 1995; Kuhn et al., 1997) and proteins (Lucas et al., 1995; Mezitt and Lucas, 1996; Jackson and Hake, 1997). This trafficking system has been postulated to be highly selective and dependent on endogenous transport proteins that evolved to shuttle specific macromolecules through plasmodesmata (Mezitt and Lucas, 1996; Jorgensen et al., 1998). A common feature of such proteins appears to be the ability to increase the plasmodesmal SEL from 1 kDa to a value in excess of 20 kDa (Mezitt and Lucas, 1996; Balachandran et al., 1997; Ishiwatari et al., 1998).

During development, leaves undergo a transition from a sink (net carbon importing) to a source (net carbon exporting) organ. The sink–source transition progresses in a basipetal pattern from the tip of the expanding leaf to its base (Turgeon, 1989). As an experimental system, the sink–source transition offers a unique opportunity to study the function of plasmodesmata in different physiological regions of the same organ. Recently, we demonstrated that phloem-mobile dyes and GFP-tagged viruses could be used to study vein classes involved in phloem unloading in leaves (Roberts et al., 1997). A further advance in imaging phloem unloading was made by Imlau et al. (1999). These authors expressed GFP (27 kDa) in source companion cells using the promoter of

§To whom correspondence should be addressed (e-mail: kopark@scri.sari.ac.uk).

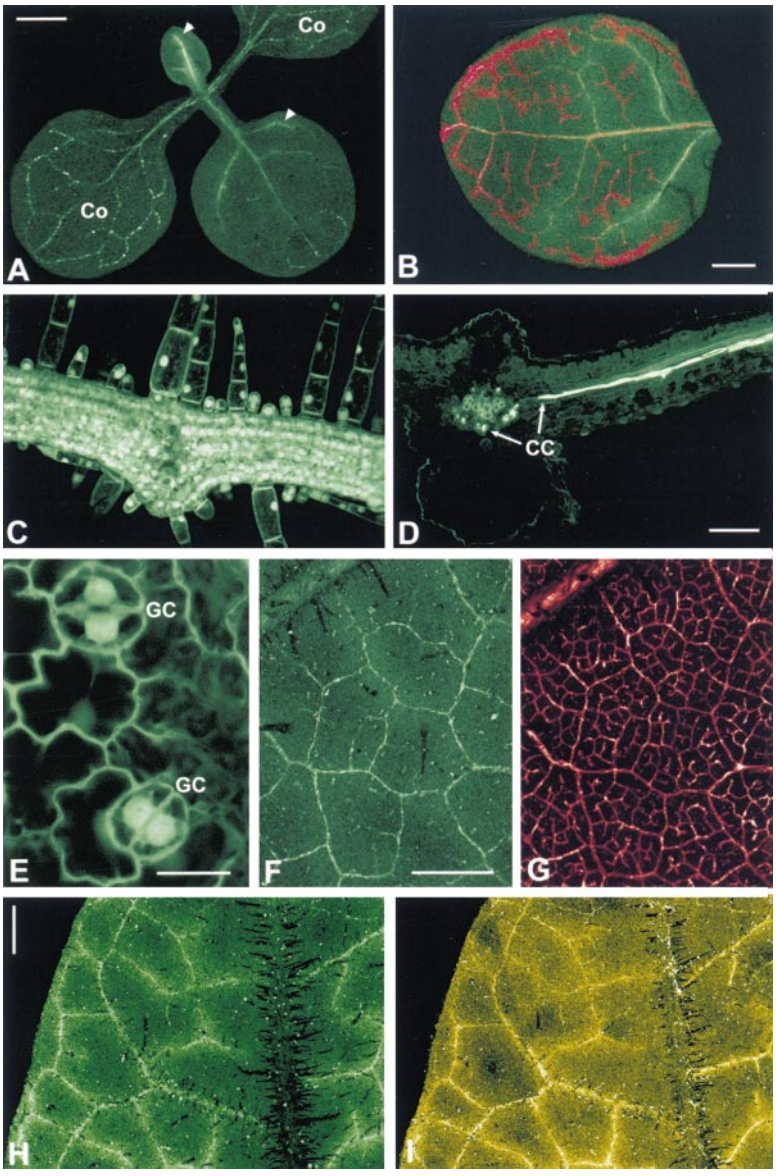

Figure 1. Transport and Unloading of GFP in Source and Sink Leaves of *Nicotiana tabacum* Plants Expressing *gfp* under Control of the *AtSUC2* Promoter

(A) Small seedling showing phloem unloading of GFP from the major veins of the first sink leaves (darts). The cotyledons (Co) show punctate fluorescence of the veins due to companion cell–specific expression of GFP. Scale, 1 mm.

(B) First sink leaf labeled with Texas red dextran to reveal the xylem. Note that unloading of GFP is restricted to the basal major veins. Scale, 0.5 mm.

(C) Transverse section of an importing sink leaf. GFP has unloaded from the phloem and entered all cell layers of the leaf, including trichomes. Scale as in (D).

(D) Transverse section of exporting source leaf. GFP is restricted to the companion cells (CC) of the phloem. The CCs are seen in both transverse and longitudinal section. Scale, 150 μm.

(E) Detail of the epidermis of an unloading sink leaf. GFP has entered epidermal cells and developing guard cell complexes. Scale, 20 μm.

(F and G) Unloading of GFP from class III veins of a sink leaf (F). The leaf was double labeled with Texas red dextran to reveal the xylem (G). Note the absence of GFP unloading from minor veins. Scale, 0.5 mm.

(H and I) A leaf unloading GFP from class III veins (H) was double labeled with carboxyfluorescein to reveal vein classes involved in the unloading of low–molecular weight solutes (I). Note the coincidence of labeling in the two images. Scale, 2 mm.

the *Arabidopsis* sucrose transport protein, *AtSUC2*. From its site of synthesis in source leaf companion cells (CCs), GFP entered the sieve elements (SEs) and was translocated to sink regions of the plant. A significant finding was that GFP was unloaded and entered the postphloem transport pathway of these sink tissues, indicating that some plant tissues may have the capacity to traffic macromolecules (see also Wang and Fisher, 1994).

In this study we examine the permeability of plasmodesmata in leaves undergoing the sink–source transition. We use transgenic tobacco plants that express GFP under control of the *AtSUC2* promoter in order to identify the sink–source transition and show that GFP, unloaded from the phloem, traffics extensively from cell to cell. Using biolistic bombardment of GFP-fusion proteins, we demonstrate that proteins of up to an M_r of 50 kDa can pass through sink leaf plasmodesmata. We show, also, that despite the large basal SEL of plasmodesmata, movement proteins are essential for the passage of viral RNA between sink cells. Finally, we demonstrate that a substantial decrease in plasmodesmal permeability occurs during the sink–source transition that is concurrent with a basipetal progression from simple to branched forms of plasmodesmata. These data provide evidence for a functional division of labor between higher-plant plasmodesmata.

Results

GFP Is Unloaded from Major Veins in Sink Tobacco Leaves

Previously, Imlau et al. (1999) demonstrated that GFP, synthesized within source leaf companion cells under control of the *AtSUC2* promoter, entered sieve elements and was translocated to sink regions of the plant. In the present study, we examined the pattern of GFP unloading in tobacco leaves in relation to the sink–source

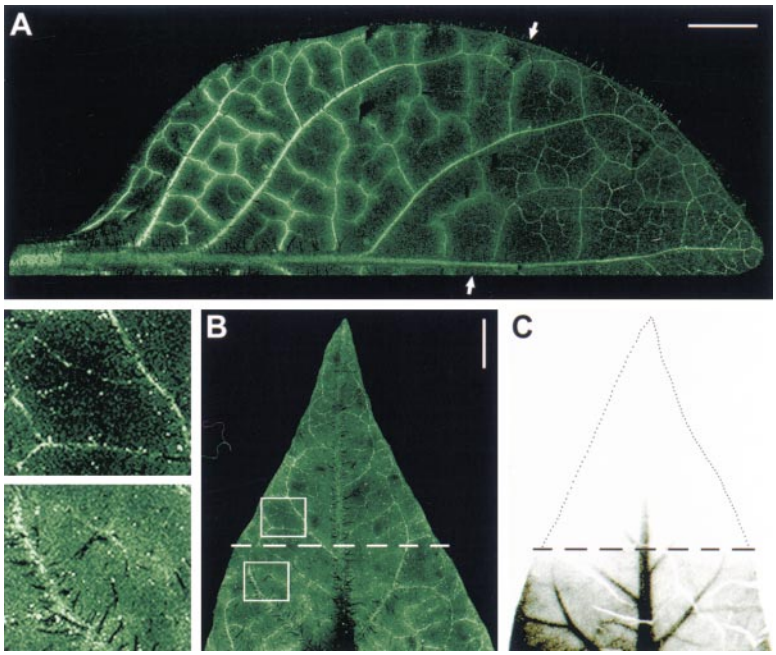

Figure 2. *AtSUC2-GFP* Tobacco Leaves Undergoing the Sink–Source Transition

(A) Montage of a series of confocal images of a leaf undergoing the sink–source transition. The basal class III veins are unloading GFP, while the apical portion of the leaf shows fluorescence from the phloem of minor veins. The arrows denote the putative position of the sink–source transition. Scale, 5 mm.

(B) Detail of the sink–source transition as revealed by GFP distribution. The lower boxed region (enlargement, lower left) shows diffuse unloading of GFP from major veins, while the upper boxed region (enlargement, upper left) shows punctate fluorescence arising from companion cells. Scale, 5 mm.

(C) Autoradiograph of the same leaf shown in (B) following labeling of the lower source leaves with $^{14}CO_2$. The sink–source transition for carbon (dashed line) matches that revealed by GFP labeling in (B). Scale as in (B).

transition. In young seedlings, viewed at low magnifications under the confocal laser scanning microscope (CLSM), differences between source and sink leaves were apparent at an early stage of development. Cotyledons displayed a highly punctate fluorescence associated with exporting veins, while the first-formed sink leaves showed diffuse symplastic unloading of GFP from major veins (Figure 1A). At higher magnifications, GFP was seen to spread from the major veins throughout mesophyll and epidermal layers of the leaf (Figures 1B, 1C, and 1E). The unloaded GFP also entered immature guard cell complexes and developing trichomes (Figures 1C and 1E). In contrast, in source leaves GFP was restricted exclusively to the phloem (Figure 1D). To follow the pattern of GFP unloading from different tobacco vein classes, the vein classification of Roberts et al. (1997) was used. In small sink leaves (<3 mm length), GFP unloading was first apparent from class I veins (the midrib) and also to a limited extent from the most basal class II veins (Figures 1A and 1B). Labeling of the leaf xylem with 3 kDa Texas red dextran showed that the vein area used in phloem unloading of GFP was small in comparison with the total vein area involved in xylem transport (Figure 1B). In older leaves (3–10 cm in length), symplastic unloading of GFP progressed from class II to class III veins (Figures 1F and 1H). However, unloading of GFP did not occur from the minor veins (classes IV and V) in any of the leaves examined (cf. Figures 1F and 1G). In leaves undergoing the sink–source transition, the unloading of GFP was restricted to basal class III veins (Figure 2A), while in the apical (source) region of these leaves GFP fluorescence became increasingly restricted to the minor veins (Figure 2A). As leaf development progressed, GFP fluorescence disappeared from epidermal and mesophyll tissues (see also Imlau et al., 1999) and remained exclusively in the CCs of minor veins (Figure 1D).

CC-Specific Expression of GFP Marks the Termination of Carbon Import

To determine whether the localization of GFP coincided with the current position of the import–export transition for carbon, the putative sink–source transition, revealed by GFP fluorescence (e.g., Figure 2A) was imaged on four intact leaves under the CLSM. The lower source leaves were then pulse-labeled with $^{14}CO_2$. The sink–source transition for carbon matched precisely the pattern of GFP distribution in the leaf, carbon import occurring in the same vein classes involved in GFP unloading (cf. Figures 2B and 2C). In a separate experiment, the phloem-mobile probe carboxyfluorescein (CF) was applied to source leaves, and its unloading pattern followed in developing sink leaves (see also Roberts et al., 1997). The unloading pattern of CF also matched precisely the pattern of GFP distribution (cf. Figures 1H and 1I). The CC-specific expression of GFP in the apical portions of leaves undergoing the sink–source transition (Figure 2A) was therefore used as an accurate marker for those regions of leaves in which carbon import had ceased.

Size Exclusion Limit of Sink Leaf Plasmodesmata

In *Nicotiana* species, mature epidermal cells in source leaves have a characteristic "jigsaw"-shaped appearance (e.g., Figures 3G–3I). This wall infolding is absent from immature epidermal cells (e.g., Figures 4D and 4E) but becomes extensive during the course of leaf development. GFP was synthesized in single epidermal cells of sink leaves following biolistic bombardment with a plasmid expressing the *gfp* gene. Intense fluorescence was detected in the initial bombarded cell and also in several cells surrounding the "hit" cell. GFP was detected in neighboring cells within 7 hr following bombardment (Figure 3A) and spread extensively following bombardment. Two days following bombardment, GFP

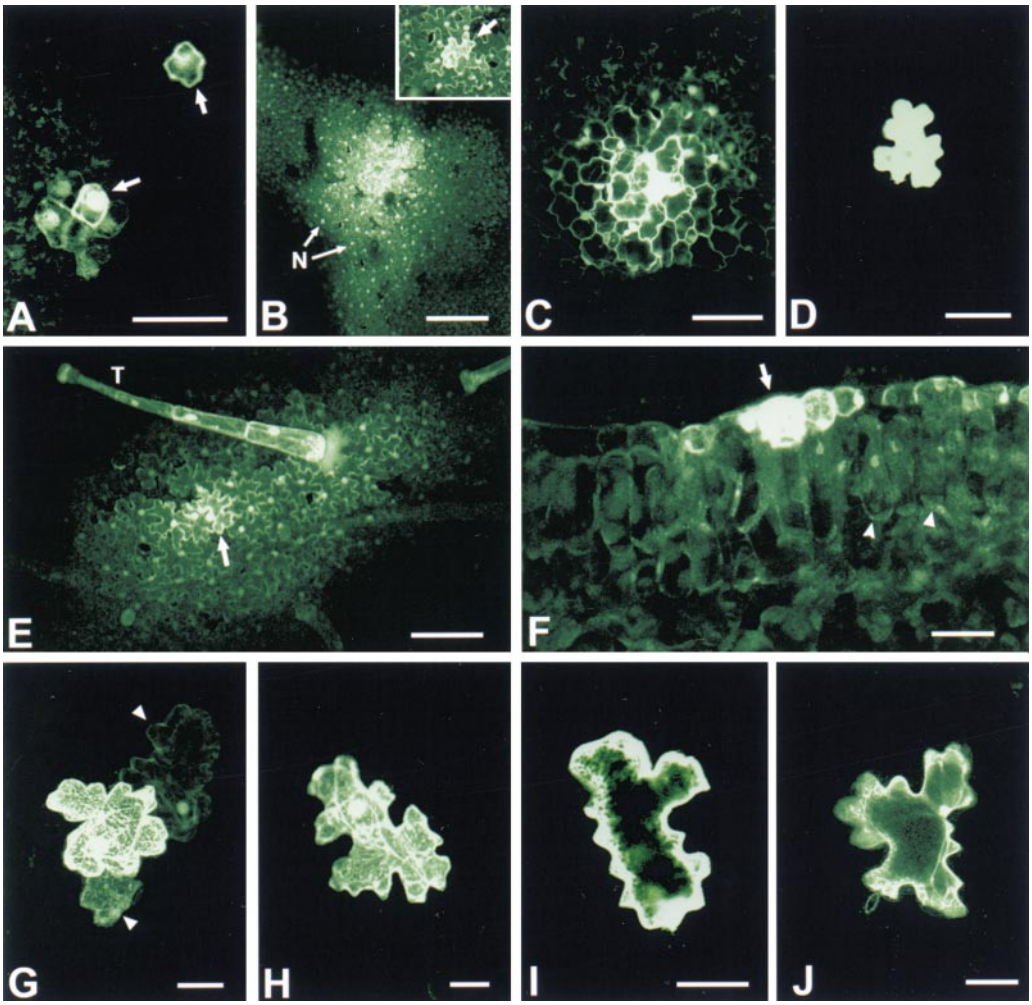

Figure 3. Biolistic Bombardment of *gfp*-Expressing Plasmids into Source and Sink Leaves of *N. clevelandii*

The bombarded cells are indicated by arrows.

(A) Movement of free GFP (27 kDa) at 7 hr following bombardment of a sink leaf. Scale, 50 μm.

(B) Extensive cell–cell movement of free GFP at 2 days following bombardment of a sink leaf. Insert shows the single bombarded cell surrounded by GFP-containing epidermal cells. Note that GFP accumulates in the nuclei (N) of cells. Scale, 200 μm.

(C) Cell–cell movement of GFP-sporamin (47 kDa) on a sink leaf. Scale, 100 μm.

(D) Nonmovement of GFP-patatin (67 kDa) on a sink leaf. Scale, 50 μm.

(E) Movement of free GFP from a single sink epidermal cell into a neighboring trichome (T). Scale, 100 μm.

(F) Movement of free GFP from a single sink epidermal cell downward into mesophyll cells (darts). Scale, 50 μm.

(G) Restricted movement of free GFP following bombardment of a source epidermal cell. Trace movement is detectable in cells immediately adjoining the bombarded cell (darts). Scale, 50 μm.

(H) Nonmovement of GFP-sporamin from a bombarded source epidermal cell. Scale, 50 μm.

(I) Nonmovement of GFP-patati (61 kDa) from a bombarded source epidermal cell. Scale, 50 μm.

(J) Nonmovement of GFP-patatin (67 kDa) from a bombarded source epidermal cell. Scale, 50 μm.

had spread into approximately 200 cells surrounding the hit cell (Figure 3B; Table 1). In sink leaves, GFP moved from single bombarded epidermal cells into developing leaf trichomes (Figure 3E) and also downward into the mesophyll (Figure 3F). In contrast, when GFP was bombarded into epidermal cells of source leaves, the spread of fluorescence was greatly restricted. However, trace movement was often observed in cells immediately adjoining the bombarded cell (Figure 3G; Table 1). Identical results were obtained with the related species *N. benthamiana* and *N. clevelandii* (data not shown). To probe the SEL of sink plasmodesmata further, the storage proteins sporamin (M_r of 20 kDa) and patatin (M_r of 40 kDa) were fused to GFP (Figure 7A) and bombarded into epidermal cells. In sink leaves, the GFP-sporamin fusion (M_r of 47 kDa) moved several cells away from the bombarded cells, but not as extensively as GFP alone (Figure 3C; Table 1). In contrast, no cell–cell movement of GFP-sporamin was observed in source leaves (Figure 3H; Table 1). A GFP-patatin fusion (M_r of 67 kDa) failed to move from cell to cell in either sink or source leaf tissues (Figures 3D and 3J; Table 1). A truncated GFP-patatin fusion was generated by removal of 56 terminal amino acids of the patatin moiety to yield a fusion protein

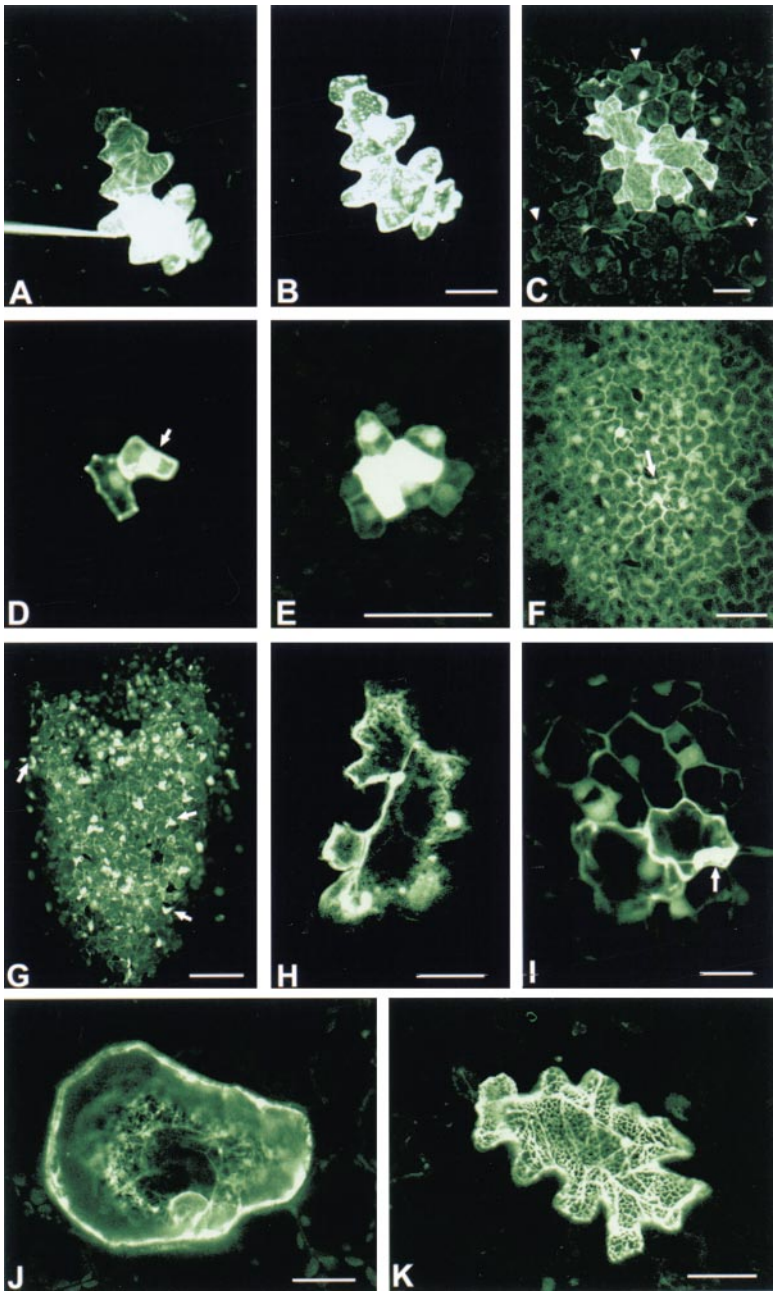

Figure 4. Microinjection of Free GFP into Source and Sink Epidermal Cells (A–F) and Bombardment of Leaves with Potato Virus X Vectors Expressing GFP as a Coat Protein Fusion (G–I), or GFP Targeted to the Endoplasmic Reticulum (J and K)

(A) Cytosolic injection of GFP into a single source epidermal cell. Scale as in (B).

(B) Same cell as (A) at 24 hr following injection shows no GFP movement. Scale, 50 μm.

(C) Trace movement of injected GFP into surrounding cells (darts) at 24 hr following injection. Scale, 50 μm.

(D) Sink epidermal cell (arrow) immediately following injection. GFP has already spread to a single neighboring cell. Scale as in (E).

(E) Same injection as (D) 2 min later. GFP has spread into a "halo" of neighboring cells. Scale, 50 μm.

(F) Extensive cell–cell movement of GFP from a single microinjected cell (arrow) into several surrounding epidermal cells at 24 hr following injection. Scale, 50 μm.

(G) Multiple-cell infection site following bombardment of PVX.GFP-CP into a single epidermal cell. Fluorescent virus aggregates (arrows) are present in each infected cell. Scale, 150 μm.

(H) Single-cell restriction of GFP following bombardment of a single source cell with a PVX vector lacking the 25 kDa protein of the triple gene block (PVX.GFP-CPΔ25). Scale, 50 μm.

(I) Cell–cell movement of free GFP following bombardment of a sink cell with PVX.GFP-CPΔ25. Note that fluorescent virus inclusions (arrow) are restricted to the bombarded cell. Scale, 25 μm.

(J and K) Restriction of GFP to the ER of a single sink (J) and source (K) cell following bombardment with PVX.Sp-GFP-KΔTGB. Scale, 20 μm in (J) and 50 μm in (K).

of 61 kDa (GFP-Patati). The truncated fusion failed to move in source (Figure 3I) or sink leaves (Table 1). The results demonstrate that proteins with an M_r of up to 47 kDa, but not as large as 61 kDa, can move freely through sink leaf plasmodesmata.

GFP Can Traffic from Cell to Cell in the Absence of Its mRNA

To examine the possibility that GFP mRNA, rather than free GFP, may have trafficked from cell to cell in sink tissues following plasmid bombardment, we microinjected a red-shifted GFP variant as the free protein into single epidermal cells of source and sink leaves of *N. clevelandii*. In source leaves, no movement of GFP occurred for up to 2 hr following injection. Twenty-four hours later, 33% of successfully injected cells failed to show any GFP movement (Figures 4A and 4B; Table 2); the remainder displayed weak GFP fluorescence in cells immediately adjoining the injected cell but not beyond (e.g., Figure 4C; Table 2). These results were similar to those obtained with biolistic bombardment using plasmids encoding GFP, in which a large proportion of cells displayed a weak GFP "halo" (Table 1). In contrast, in sink leaves 82% of the injected cells showed extensive cell–cell movement of GFP (Figure 4F; Table 2), a significant proportion of total injections (30%) showing immediate movement to adjoining cells (Figures 4D and 4E; Table 2). As expected, fluorescence from the injected

Table 1. Cell-to-Cell Movement of GFP Fluorescence from Epidermal Cells Bombarded with Plasmid Constructs

Protein Expressed by Bombarded Plasmid	Estimated Size of GFP Fusion (kDa)	Total No. of Hits Observed		No. of Single Cells		No. of Halos[a]		Avg. No. of Cells in Halo	
		Sink	Source	Sink	Source	Sink	Source	Sink	Source
GFP	27	20	34	0	4	20	30	193	3
GFP-sporamin	47	23	32	0	29	23	3	57	1
GFP-patati	61	35	18	28	18	7	0	2	—
GFP-patatin	67	24	25	22	25	2	0	1	—

[a] A halo was defined as the total number of GFP-containing cells surrounding the bombarded cell.

GFP was faint in comparison with plasmid-encoded GFP, due to the lack of synthesis of GFP following injection.

Viral RNA Cannot Traffic in Sink Leaves in the Absence of Movement Proteins

Because of the large basal SEL of sink leaf plasmodesmata, we tested the hypothesis that viral RNA might traffic in sink regions of the leaf in the absence of viral movement proteins. In potato virus X, three overlapping gene products, called the triple gene block (TGB), encode proteins essential for cell–cell movement of the virus (Petty and Jackson, 1990; Beck et al., 1991; Santa Cruz et al., 1998). One of these, the 25 kDa TGB protein, has been shown to modify plasmodesmal SEL (Angell et al., 1996) and is essential for cell–cell spread of PVX (Santa Cruz et al., 1998). Previously, we showed that GFP could be fused to the CP of PVX to produce a functional virus that carried a GFP "overcoat" (PVX.GFP-CP, Figure 7B; Santa Cruz et al., 1996). In the present study, we constructed a mutant PVX genome in which GFP was fused to the viral coat protein but in which the 25 kDa gene was deleted. This mutant virus (PVX.GFP-CPΔ25; Figure 7B) was inoculated onto both sink and source leaves of *N. clevelandii*. On source leaves infected with PVX.GFP-CP, the viral infection sites were multicellular, each infected cell containing an aggregate of fluorescent virus particles (Figure 4G). In contrast, when source leaves were infected with PVX.GFP-CPΔ25 the virus was restricted to single epidermal cells (Figure 4H). In sink leaves infected with PVX.GFP-CPΔ25, fluorescent virus aggregates were found in single epidermal cells, but in this case the GFP was also detected in several cells around the infected cell (Figure 4I). The complete absence of fluorescent virus in adjoining cells indicated that the free GFP produced during viral replication, but not viral RNA, had trafficked out of the infected cell.

Table 2. Cell-to-Cell Movement of Free GFP after Microinjection into Sink and Source Leaves

	Total No. of Injections	Spontaneous GFP Movement	GFP Movement after 24 hr	No GFP Movement after 24 hr
Source cells	9	0	6[a]	3
Sink cells	30	9	18[b]	6

[a] Movement into adjacent cells only.
[b] Extensive cell-to-cell movement (movement up to six cells radially from injected cell).

Plasmodesmal Structure in Source versus Sink Regions of the Leaf

To examine the structure of plasmodesmata during the sink–source transition, leaf samples were taken from each leaf on *AtSUC2* transgenic tobacco plants expressing GFP. The sink–source transition was demarcated by the change in appearance of vein classes that were unloading GFP and those that showed CC-specific expression of GFP (see above). In the case of transition leaves, tissue samples were taken from either side of the transition zone (Figure 5).

Counts of plasmodesmal types (simple versus branched) revealed a marked reduction in the proportion of simple plasmodesmata in source tissues during the progression of the sink–source transition (Figure 5). Tissue samples taken at the base of the leaf showed predominantly

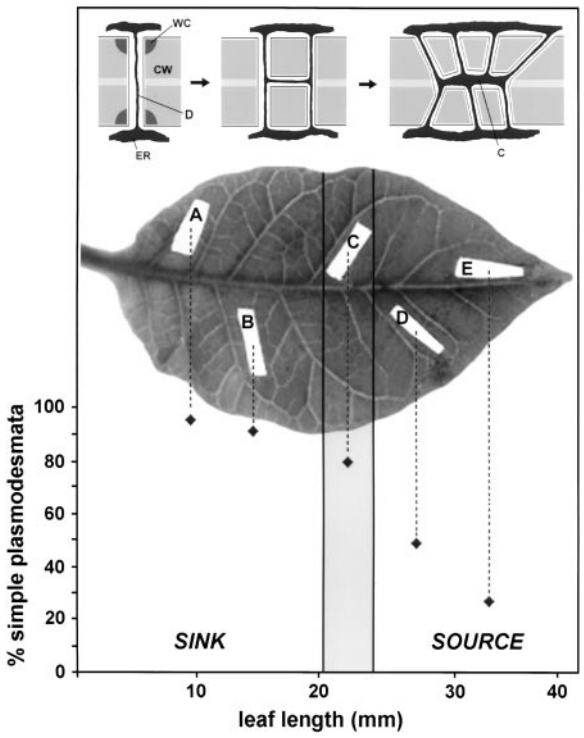

Figure 5. The Sink–Source Transition Is Accompanied by a Structural Change from Simple to Branched Forms of Plasmodesmata

The graph (bottom) shows the percentage of simple plasmodesmata found in different sectors of the leaf. The sink–source transition is shown within the shaded region. The regions (A)–(E) are shown in Figure 6. C, central cavity; CW, cell wall; D, desmotubule; ER, endoplasmic reticulum; WC, wall collar.

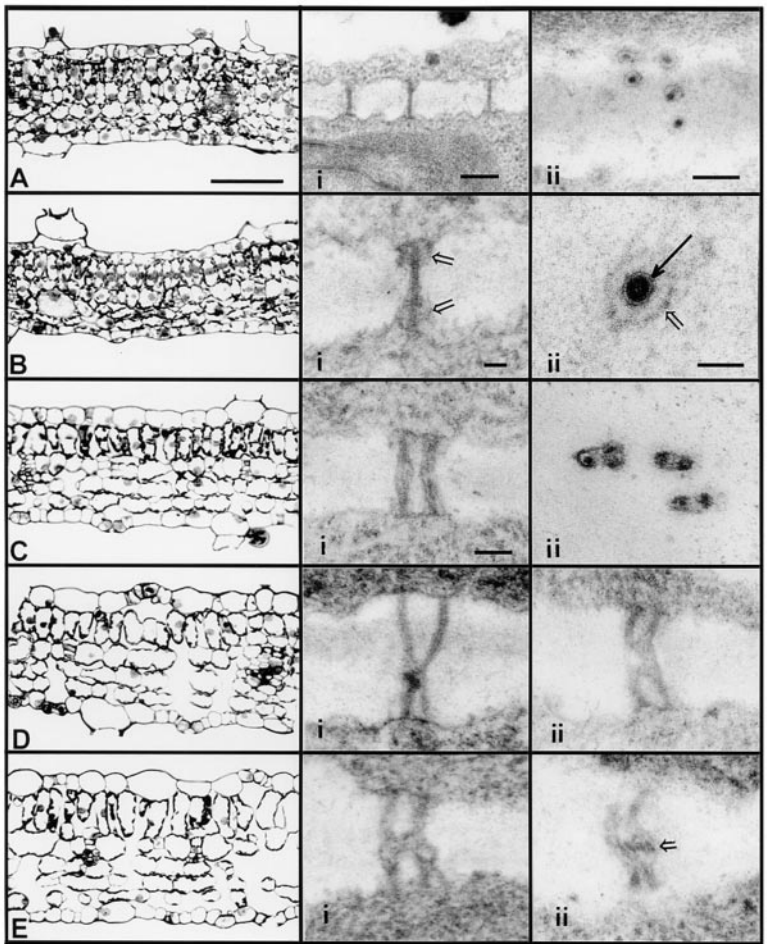

Figure 6. Transverse Sections Taken through a Leaf Undergoing the Sink–Source Transition

The sections were sampled from the regions shown in Figures 5A–5E. The electron micrographs show the appearance of plasmodesmata in the different sectors of the leaf.

(A) Simple plasmodesmata in longitudinal (i) and transverse (ii) orientations. Scale, 200 nm.

(B) Simple plasmodesmata. A conspicuous wall collar (open arrows) is evident in both longitudinal (i) and transverse (ii) orientations (closed arrow points to plasma membrane). Scale, 50 nm.

(C) Within the region of the sink–source transition, "pairing" of simple plasmodesmata can be seen in longitudinal (i) and transverse (ii) orientations. Scale, 100 nm.

(D) Source plasmodesmata, showing "H" shaped configurations. Scale as in (C).

(E) Branched plasmodesmata in the apical (source) region of the leaf showing central cavities (arrow). Scale as in (C).

simple plasmodesmata, while those at the tip were mainly branched (Figures 5 and 6). In tannic acid–stained samples, studied by electron microscopy, the simple plasmodesmata had conspicuous wall collars surrounding the neck of the pore (Figures 6A and 6B). Within the region of the sink–source transition, "pairs" of simple plasmodesmata were observed routinely in both longitudinal (Figure 6C,i) and oblique (Figure 6C,ii) sections of the wall, giving rise to "H"-shaped plasmodesmal branching patterns (Figures 6D and 6E). Branched plasmodesmata also displayed conspicuous median cavities (Figure 6E). Unlike the simple plasmodesmata in sink tissues, the branched plasmodesmata found in source regions of the leaf did not display electron-dense wall collars (Figures 6D and 6E).

GFP Cannot Traffic through the Desmotubule

Because of the structural differences between simple and branched plasmodesmata, we examined the possibility that the desmotubule may provide a possible transport pathway between leaf cells (see Gamalei et al., 1994; Figure 5). Previously, we demonstrated that GFP can be targeted to the endoplasmic reticulum of leaf cells using a PVX vector that expressed GFP fused to a patatin signal peptide and a KDEL retention signal (Boevink et al., 1996). In the present study, we employed a PVX vector that lacked the TGB proteins but which expressed GFP carrying the sporamin signal peptide and KDEL retention signal (PVX.sp-GFP-KΔTGB; Figure 7B). As the TGB proteins are essential for cell–cell movement of PVX (Santa Cruz et al., 1998), ER-targeted GFP was confined to single cells. We examined whether GFP, present within the lumen of the cortical ER, was capable of trafficking from the infected cell to the neighboring cells via the connecting desmotubules of plasmodesmata. Five days after infection, ER fluorescence remained intense within the ER of the inoculated cells due to continued viral replication and synthesis of GFP (Figures 4J and 4K). Cytoplasmic streaming within these cells was also evident (data not shown), indicating that the cells had remained viable over this period. However, no GFP was detected within the cortical ER of adjoining cells of either sink or source leaf tissues (Figures 4J and 4K). Thus, the desmotubule is not a functional pathway for GFP trafficking through either simple or branched plasmodesmata.

Discussion

During the sink–source transition in leaves, a major change occurs in the permeability of plasmodesmata. In developing sink leaves, plasmodesmata allowed the unrestricted movement of phloem-unloaded GFP (Imlau et al., 1999). The pattern of GFP unloading was identical

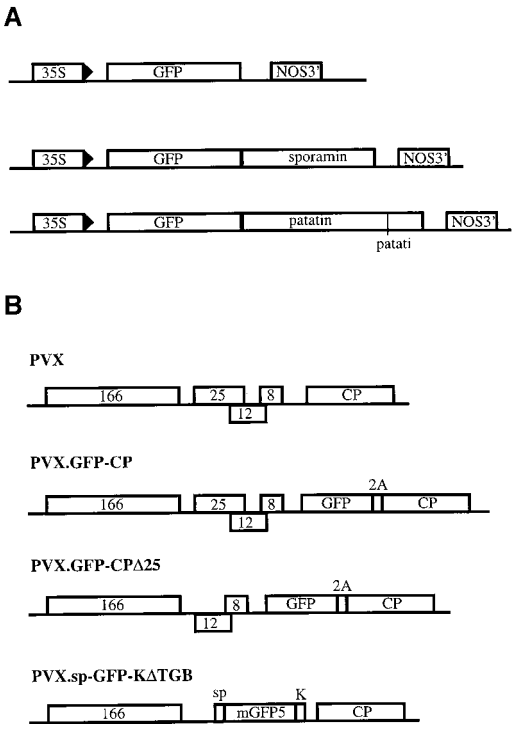

Figure 7. Transient Expression Vectors (A) and Viral Clones (B) Used for Microprojectile Bombardment of Leaves

to that found for the low–molecular weight probe CF, suggesting that macromolecules and solutes are unloaded from the phloem by the same vein classes.

It appears that a range of macromolecules may be able to move through plasmodesmata in the postphloem pathway in sink tissues. Wang and Fisher (1994) showed that dextrans (M_r of 10 kDa) applied to the postphloem crease region of the wheat grain were capable of moving from cell to cell. More recently, Fisher (unpublished data) has shown that dextrans and proteins in the size range of 10–60 kDa when microinjected into a single SE of the wheat grain, via a severed aphid stylet, were capable of postphloem transport through crease tissues. The nonspecific movement of a range of "xenobiotic" macromolecules through sink plasmodesmata makes it unlikely that their cell–cell movement requires a specific interaction with plasmodesmal proteins or transporters (e.g., Lucas, 1995). Instead, it is more likely that the cytoplasmic sleeve of plasmodesmata in sink leaves can accommodate the passage of macromolecules with an upper size limit of 50–60 kDa. In contrast, source regions of the leaf showed restricted cell–cell movement of GFP. This is consistent with numerous previous reports that macromolecules do not move readily through source leaf plasmodesmata, unless the latter are modified by viral MPs (Wolf et al., 1989, 1991; Deom et al., 1990) or some other form of endogenous movement factor (Mezitt and Lucas, 1996). When we targeted GFP to the cortical ER of single cells, no fluorescence appeared in the ER of adjoining cells. Thus, if intercellular protein trafficking does occur through the desmotubule, it must be restricted to molecules smaller than GFP.

The massive decrease in plasmodesmal permeability during the sink–source transition was correlated closely with a developmental change from simple to branched plasmodesmata. In higher plants, the transition from simple to branched plasmodesmata is a normal feature of development and occurs in both leaves (Ding et al., 1992; Itaya et al., 1998) and roots (Gunning, 1978; Seagull, 1983; Zhu et al., 1998). However, the very high SEL of simple plasmodesmata in leaves has not previously been recorded. Previous studies, employing microinjection (Wolf et al., 1989; 1991; Deom et al., 1990) and biolistic bombardment (Ding et al., 1995; Itaya et al., 1998), have suggested that simple plasmodesmata in developing tobacco leaves have a low SEL. Contrary to these reports, we found that GFP, whether microinjected or synthesized following bombardment with a GFP-encoding plasmid, resulted in extensive cell–cell movement of the 27 kDa protein in sink leaves. Unlike dextrans, GFP cannot be broken down by cells to produce smaller fluorescent moieties without loss of fluorescence (Dopf and Horiagan, 1996). Thus, we are confident that the fluorescence seen in surrounding cells was not due to degradation of GFP into smaller, symplastically mobile units. In previous developmental studies of plasmodesmata, the exact position of the sink–source transition was not determined (Itaya et al., 1998). This point is crucial when considering the movement of dyes injected into leaf mesophyll cells and may explain some of the discrepancies in the literature concerning the ability of dyes of different molecular masses to move between cells. Our current data suggest that estimates of the permeability of plasmodesmata will depend on whether sink or source tissues are examined.

It has been suggested that the simple plasmodesmata in developing leaves are not targeted by viral MPs (Itaya et al., 1997, 1998). However, branched plasmodesmata in transgenic plants expressing the TMV MP (Ding et al. 1992), and also plasmodesmata in source leaves infected with wild-type TMV (Tomenius et al., 1987), accumulate MP in the central cavity of the pore. Similarly, MPs from a range of viruses, fused to GFP, have been shown to target the central cavity of plasmodesmata during viral movement (Oparka et al., 1996, 1997; Itaya et al., 1997; Ryabov et al. 1997; Blackman et al., 1998). Because of the high natural SEL of sink plasmodesmata, and because viral MPs do not appear to accumulate in simple plasmodesmata, we tested the hypothesis that viruses may not require MPs for passage from cell to cell in sink tissues. Infection of cells in sink leaves with an MP-defective PVX construct showed that free GFP, but not viral RNA, moved out of infected cells in the absence of MP. Thus, it appears that an interaction between viral RNA and MP is also required in simple plasmodesmata before movement of the viral genome can occur.

Although viral RNA did not move through simple plasmodesmata in sink leaves, this observation does not preclude the possibility that small RNA molecules ($<$50 kDa) might move through plasmodemata in sink tissues. During the phenomenon of systemic acquired silencing, a systemic signal is transmitted from source leaves to sink leaves, inducing gene silencing in cells of the sink leaf (Voinnet and Baulcombe, 1997; Jorgensen et al., 1998). The nature of this systemic signal is presently unknown, but it has been suggested to be a small copy

RNA (cRNA) molecule that is translocated through the phloem (Jorgensen et al., 1998). Interestingly, the initial pattern of gene silencing in sink tobacco leaves appears in the vicinity of class III veins (see Palauqui et al., 1997), suggesting that the systemic signal exits the phloem from the same vein class involved in unloading GFP, solutes, and viruses (see also Roberts et al., 1997). Given the large basal SEL of sink cells, it is possible that small cRNA molecules could move freely through the plasmodesmata in the postphloem pathway of sink tissues, initiating cosuppression in all developing cells.

To date, studies of plasmodesmata have concentrated on physiological, rather than developmental, modulation of SEL. For example, plasmodesmal permeability has been shown to increase substantially in response to metabolic inhibitors (Tucker, 1993; Cleland et al., 1994; Wright and Oparka, 1997), anaerobic stress (Cleland et al., 1994), osmotic stress (Schulz, 1995), and inhibitors of actin polymerization (Ding et al., 1996). One explanation of these data is that some physiological traumas may restore in branched plasmodesmata the "juvenile" permeability normally associated with simple plasmodesmata. In lower plants, such as mosses (Cook et al., 1997), and ferns (Gunning, 1978; Tilney et al., 1990) simple plasmodesmata predominate. Simple plasmodesmata occur in many groups of algae (Raven, 1997), although in the green alga *Chara corallina*, plasmodesmal branching occurs from existing simple plasmodesmata (Franceschi et al., 1994). Macromolecular trafficking through plasmodesmata has been demonstrated in the alga *Nitella* (Kikuyama et al., 1992), proteins up to 45 kDa moving from one cell to the next while retaining their biological function. The change from simple to branched plasmodesmata that occurs during leaf development, coupled to the corresponding decrease in SEL, may be a case of "ontogeny recapitulating phylogeny" (i.e., more primitive [simple] plasmodesmata facilitate macromolecular trafficking, while more advanced [branched] plasmodesmata restrict the nonspecific movement of macromolecules). It is perhaps significant that in the phloem unloading regions of wheat (Wang et al., 1995) and rice (Oparka and Gates, 1981) caryopses, and in transverse walls of developing roots (Seagull, 1983; Zhu et al., 1998), most of the plasmodesmata that connect cells in the postphloem pathway are simple pores.

We suggest that the difference in plasmodesmal permeability between source and sink leaf tissues may reflect the plant's need to control the intercellular movement of macromolecules during leaf development. The concept of macromolecular trafficking, as attributed to higher-plant plasmodesmata (Lucas et al., 1993), implies that proteins require a specific chaperone-based mechanism to facilitate their passage through the plasmodesmal pore (Mezitt and Lucas, 1996). This requirement does not appear to exist in sink tissues where nonspecific passage of proteins up to 50 kDa is possible via the cytoplasmic sleeve of plasmodesmata. Downregulation of plasmodesmal conductance in source leaf tissues during the export phase may be a mechanism that ensures the strict regulation of intercellular transport, the branched plasmodesmata acting as "molecular sieves" to prevent nonspecific cell–cell movement in the source leaf. Thus, in source tissues, only those macromolecules able to modify plasmodesmal SEL, or those that possess specific chaperone proteins to facilitate their passage through plasmodesmata (Lucas, 1995; Mezitt and Lucas, 1996), will gain access to the phloem. If this model is correct, then molecular discrimination at the level of plasmodesmata may occur in source tissues only. However, it should be noted that specific proteins synthesized within the CCs of source leaves can be transported into sieve elements and translocated to sink tissues where they will be unloaded (Imlau et al., 1999). Oparka and Turgeon (1999) have likened the SE–CC complex in source leaves to a "passport control center" that determines the nature of molecules allowed to enter the phloem. Once in the SE, the fate of such molecules will be determined by the translocation stream. The indiscriminate exit of a range of macromolecules through the postphloem pathway in sink tissues, coupled to the large basal SEL of sink plasmodesmata, may be a mechanism that facilitates the rapid entry of macromolecules into growing sink cells.

Experimental Procedures

Plant Material

All plants were grown from seed in a heated glasshouse and used for experiments when they were between 15 and 60 days old.

Imaging Intact Plants

Small leaves of *AtSUC2-GFP* transgenic plants (Imlau et al., 1999) were mounted, abaxial surface upward, in distilled water and covered with a coverslip. The leaves were imaged using a confocal laser scanning microscope equipped with Nikon X1-X4 long-working distance lenses. In the case of larger sink leaves (3–10 cm), the leaves were detached from the plant and stuck down to a glass slide with double-sided adhesive tape. The abaxial surface was then "mapped" using a X1 or X2 lens, and the images were subsequently reconstructed using Photoshop software (Adobe, Mountain View, CA; see Roberts et al., 1997). In some instances, major veins expressing GFP were excised from the leaf, mounted in agar, and sectioned transversely using a Vibroslice (Campden Instruments; see Santa Cruz et al., 1998).

Phloem and Xylem Transport

Phloem transport was imaged on intact plants using the fluorescent probe carboxyfluorescein (CF), exactly as described by Roberts et al. (1999). To image xylem transport, intact sink leaves expressing GFP, or sink leaves that had translocated CF, were excised and the petiole immersed in a solution of 3 kDa Texas red dextran for 5–10 min (see also Roberts et al., 1997).

$^{14}CO_2$ Labeling

Developing sink leaves from four plants were imaged under the confocal microscope while still attached to the plant to determine the putative position of the sink–source transition, revealed by GFP expression. The position of the sink–source transition was then marked on each leaf. Three source leaves on each plant were labeled with $^{14}CO_2$ for 30 min as described by Roberts et al. (1997). The plants were then left to translocate carbon-14 for a further 2 hr chase period. The sink leaves were then removed, freeze dried, and mounted for autoradiography (Roberts et al., 1997).

Construction of Transient Expression Vectors

Standard techniques were used throughout (Sambrook et al., 1989). The pRTL2-based plasmids used for the bombardment studies are shown in Figure 7A. pRTL2.GFP-sporamin was created by PCR amplification of the GFP coding sequence from pRTL2.GFP (Itaya et al., 1997) and the mature sporamin protein coding sequence from pIM023 (Hattori et al., 1985) using primers that introduced appropriate restriction sites, then digestion and ligation of the fragments and cloning the resulting fragment into pRTL2 (Carrington and Freed, 1990; Restrepo et al., 1990). The primer sequences for

GFP were CTACCATGGTGAGCAAGGGCGA (primer 1) and TCATTC GAACTTGTACAGCTC (primer 2), and for sporamin they were ATC TTCGAATCCTCTGAAACTCCA and CTTGGATCCTTACACATCGG TAG. pRTL2.GFP-patatin was created in the same way. The mature patatin protein coding sequence was amplified from pPatB2 (Stiekema et al., 1988). The primers used were as follows: primer 1 (above) and TCACGGCCGCTTGTACAGCTC for GFP; TCACGGCCG AAGTTGGAAGAAATG and ATGGTACCTTAATGAGAAGCTTTG for patatin. pRTL2.GFP-patati was created using the NsiI site, which is 196 bp from the 3′ end of the patatin sequence. The full-length fusion clone was cut with NsiI, treated with T4 DNA polymerase, and the clone was religated. This introduced a frameshift in the coding sequence, and a stop codon was in-frame six codons downstream. The resulting fusion protein was estimated to have a molecular weight of 61 kDa.

Construction of Viral Vectors

The viral genomes contained within the plasmids used are depicted in Figure 7B. The plasmid pTXS7 (M. Longstaff, unpublished data), which carries a full-length cDNA of PVX strain DX under the transcriptional control of the 35S promoter, was used as the basis for plasmids carrying PVX vector constructs. pCaX.GFP-CP and pCaX.sp-mGFP5-K were prepared by replacing the BamHI/SpeI fragment in pTXS7 with the corresponding sequences from pTXS.GFP-CP (Santa Cruz et al., 1996) and pTXS.sp-mGFP5-K, respectively. pTXS.sp-mGFP5-K was derived from pTXS.sp-GFP-K (Boevink et al., 1999) by replacement of the wild-type GFP with m-GFP5 (Siemering et al., 1996). pCaX.GFP-CPΔ25 is identical to pCaX.GFP-CP with the exception that a 4 bp deletion has been introduced in the gene encoding the 25 kDa protein. After inoculation, the viral constructs were referred to using the suffix PVX instead of pCaX (Figure 7B).

Microprojectile Bombardment of Leaves

Plasmid DNAs were introduced into *Nicotiana clevelandii* leaf cells by particle bombardment. The method was essentially as described by Gal-On et al. (1997). Approximately 50 ng of plasmid DNA was mixed with 0.55 mg of 1 mm gold particles in ethanol and made up to a final volume of 16 ml with ethanol. Two millilters of the DNA/gold mixture was loaded onto the grid of a discharge assembly and left until the ethanol evaporated. Beginning with a source leaf and progressing to sink leaves, three to four bombardments were made before reloading the grid. Bombarded leaves were observed under the CSLM after 1–3 days.

Microinjection

A highly fluorescent, red-shifted GFP variant (rEGFP; Clontech Inc, Palo Alto, CA) was injected into epidermal cells of source and sink leaves of *N. clevelandii* at a concentration of 1 mg/ml. Microinjection was performed using a modified pressure probe to minimize vacuolar impalement (see Oparka et al., 1997). Images of injected cells were collected immediately after injection and also at 24 hr following injection.

Light and Electron Microscopy

Leaf samples from selected leaves of *AtSUC2-GFP* tobacco plants undergoing the sink–source transition were excised, then fixed in 5% glutaraldehyde in 0.2 M PIPES buffer (pH 8.0), containing 1% tannic acid to enhance fixation and membrane definition (Mizuhira and Futaesaku, 1971, 1972; Simionescu and Simionescu, 1976), then processed through alcohol into Araldite resin (Agar Scientific Ltd., UK).

Counts of Plasmodesmata

Plasmodesmata were counted in a 35 μm length of leaf blade section. Only complete profiles of plasmodesmata that transected a shared cell wall or extended from one plasma membrane to beyond the middle lamella of the wall were counted. No counts were done of transverse or oblique sections through plasmodesmata.

Acknowledgments

This work was supported by the Scottish Office Agriculture, Environment and Fisheries Department (SOAEFD to K. J. O.), the Binational Agricultural Research Development Fund (BARD IS-2636-95 to B. L. E.), and the Deutsche Forschungsgemeinschaft (SFB47/A3 to N. S.). P. B. was supported by an EMBO fellowship. The authors would like to thank James Carrington (Washington State University, Pullman) for pRTL2, Biao Ding (Oklahoma State University, Stillwater) for pRTL2.GFP, and Marion Longstaff (Axis Genetics Plc., Cambridge) for pDX12.

Received March 17, 1999; revised May 10, 1999.

References

Angell, S.M., Davies, C., and Baulcombe, D.C. (1996). Cell-to-cell movement of potato virus X is associated with a change in the size-exclusion limit of plasmodesmata in trichome cells of *Nicotiana clevelandii*. Virology *216*, 197–201.

Balachandran, S., Xiang, Y., Schobert, C., Thomson, G.A., and Lucas, W.J. (1997). Phloem sap proteins from *Cucurbita maxima* and *Ricinus communis* have the capacity to traffic cell to cell through plasmodesmata. Proc. Natl. Acad. Sci. USA *94*, 14150–14155.

Beck, D.L., Guilford, P.J., Voot, D.M., Andersen, M.T., and Forster, R.L.S. (1991). Triple gene block proteins of white clover mosaic potexvirus are required for transport. Virology *183*, 695–702.

Blackman, L,M., Boevink, P., Santa Cruz, S., Palukaitis, P., and Oparka, K.J. (1998). The movement protein of cucumber mosaic virus traffics into sieve elements in minor veins of *Nicotiana clevelandii*. Plant Cell *10*, 525–537.

Boevink, P., Santa Cruz, S., Hawes, C., Harris, N., and Oparka, K.J. (1996). Virus-mediated delivery of the green fluorescent protein to the endoplasmic reticulum of plant cells. Plant J. *10*, 935–941.

Boevink, P.B., Martin, B., Oparka, K.J., Santa Cruz, S., and Hawes, C. (1999). Transport of virally expressed green fluorescent protein through the secretory pathway in tobacco leaves is inhibited by cold shock and brefeldin A. Planta, in press.

Burnell, J.N. (1988). An enzymatic method for measuring the molecular weight exclusion limit of plasmodesmata of bundle sheath cells of C4 plants. J. Exp. Bot. *39*, 1575–1580.

Carrington, J.C., and Freed, D.D. (1990). Cap-independent enhancement of translation by a plant potyvirus 5′ nontranslated region. J. Virol. *64*, 1590–1597.

Carrington, J.C., Kasschau, K.D., Mahajan, S.K., and Schaad, M.C. (1996). Cell-to-cell and long-distance transport of viruses in plants. Plant Cell *8*, 1669–1681.

Cleland, R.E., Fujiwara, T., and Lucas, W.J. (1994). Plasmodesmal-mediated cell-to-cell transport in wheat roots is modulated by anaerobic stress. Protoplasma *178*, 81–85.

Cook, M.E., Graham, L.E., Botha, C.E.J., and Lavin, C.A. (1997). Comparative ultrastructure of plasmodesmata of *Chara* and selected bryophytes: towards an elucidation of the evolutionary origin of plant plasmodesmata. Amer. J. Bot. *84*, 1169–1178.

Deom, C.M., Schubert, K.R., Wolf, S., Holt, C., Lucas, W.J., and Beachy, R.N. (1990). Molecular characterisation and biological function of the movement protein of tobacco mosaic virus in transgenic plants. Proc. Natl. Acad. Sci. USA *87*, 3284–3288.

Ding, B., and Lucas, W.J. (1996). Secondary plasmodesmata: biogenesis, special functions, and evolution. In Membranes: Specialised Functions in Plants, M. Smallwood, P. Knox, and D. Bowles, eds. (Oxford: BIOS Scientific Publishers Inc.), pp. 489–506.

Ding, B., Haudenshield, J.S., Hull, R.J., Wolf, S., Beachy, R.N., and Lucas, W.J. (1992). Secondary plasmodesmata are specific sites of localization of the tobacco mosaic virus movement protein in transgenic tobacco plants. Plant Cell *4*, 915–928.

Ding, B., Li, Q.-b., Nguyen, L., Palukaitis, P., and Lucas, W.J. (1995). Cucumber mosaic virus 3a protein potentiates cell-to-cell trafficking of CMV vRNA in tobacco plants. Virology *207*, 345–353.

Ding, B., Kwon, M.O., and Warnberg, L. (1996). Evidence that actin filaments are involved in controlling the permeability of plasmodesmata in tobacco mesophyll. Plant J. *10*, 157–164.

Dopf, J., and Horiagan, T. (1996). Deletion mapping of the *Aequorea victoria* green fluorescent protein. Gene *173*, 39–44.

Ehlers, K., and Kollmann, R. (1996). Formation of branched plasmodesmata in regenerating *Solanum nigrum* protoplasts. Planta *199*, 126–138.

Epel, B., Padgett, H.S., Heinlein, M., and Beachy, R.N. (1996). Plant virus movement protein dynamics probed with a movement protein fused to GFP. Gene *173*, 75–79.

Erwee, M.G., and Goodwin, P.B. (1985). Symplast domains in extrastelar tissues of *Egeria densa* Planch. Planta *163*, 9–19.

Fenczik, C.S., Epel, B.L., and Beachy, R.N. (1996). Role of plasmodesmata and viral movement protein in spread of plant viruses. In Plant Gene Research: Signal Transduction in Plant Development. (New York: Springer-Verlag Wein), pp. 249–279.

Franceschi, V.R., Ding, B., and Lucas, W.J. (1994). Mechanism of plasmodesmata formation in characean algae in relation to evolution of intercellular communication in higher-plants. Planta *192*, 347–358.

Fujiwara, T., Giesman-Cookmeyer, D., Ding, B., Lommel, S.A., and Lucas, W.J. (1993). Cell-to-cell trafficking of macromolecules through plasmodesmata potentiated by the red clover necrotic mosaic virus movement protein. Plant Cell *5*, 1783–1794.

Gal-On, A., Meiri, E., Elman, C., Gray, D.J., and Gaba, V. (1997). Simple hand-held devices for the efficient infection of plants with viral-encoding constructs by particle bombardment. J. Virol. Methods *64*, 103–110.

Gamalei, Y.V., van Bel, A.J.E., Pakhomova, M.V., and Sjutkina, A. (1994). Effects of temperature on the conformation of the endoplasmic reticulum and on starch accumulation in leaves with the symplastic minor vein configuration. Planta *194*, 443–453.

Gilbertson, R.L., and Lucas, W.J. (1996). How do viruses traffic on the "vascular highway"? Trends Plant Sci. *1*, 260–268.

Goodwin, P.B. (1983). Molecular size limit for movement in the symplast of the *Elodea* leaf. Planta *157*, 124–130.

Gunning, B.E.S. (1978). Age-related and origin-related control of the numbers of plasmodesmata in cell walls of developing *Azolla* roots. Planta *143*, 121–144.

Hattori, T., Nakagawa, T., Maeshima, M., Nakamura, K., and Asahi, T. (1985). Molecular cloning and nucleotide sequence of cDNA for sporamin, the major soluble protein of sweet potato tuberous roots. Plant Mol. Biol. *5*, 313–320.

Hepler, P.K. (1982). Endoplasmic reticulum in the formation of the cell plate and plasmodesmata. Protoplasma *111*, 121–133.

Imlau, A., Truernit, E., and Sauer, N. (1999). Cell-to-cell and long-distance trafficking of the green fluorescent protein in the phloem and symplastic unloading of the protein into sink tissues. Plant Cell *11*, 309–322.

Ishiwatari, Y., Fujiwara, T., McFarland, K.C., Nemoto, K., Hayashi, H., Chino, M., and Lucas, W.J. (1998). Rice phloem thioredoxin has the capacity to mediate its own cell-to-cell transport. Planta *205*, 12–22.

Itaya, A., Hickman, H., Bao, Y., Nelson, R., and Ding, B. (1997). Cell-to-cell trafficking of cucumber mosaic virus movement protein: green fluorescent protein produced by biolistic gene bombardment in tobacco. Plant J. *12*, 1223–1230.

Itaya, A., Woo, Y.-M., Masuta, C., Bao, Y., Nelson, R., and Ding, B. (1998). Developmental regulation of intercellular protein trafficking through plasmodesmata in tobacco leaf epidermis. Plant Physiol. *118*, 373–385.

Jackson, D., and Hake, S. (1997). Morphogenesis on the move: cell-to-cell trafficking of plant regulatory proteins. Curr. Opin. Genet. Dev. *7*, 495–500.

Jorgensen, R., Atkinson, R.G., Forster, R.L.S., and Lucas, W.J. (1998). An RNA-based information superhighway in plants. Science *279*, 1486–1487.

Kikuyama, M., Hara, Y., Shimada, K., Yamamoto, K., and Hiramoto, Y. (1992). Intercellular transport of macromolecules in *Nitella*. Plant Cell Physiol. *33*, 413–417.

Kollmann, R., and Glockmann, C. (1985). Studies on graft unions. I. plasmodesmata between cells of plants belonging to different unrelated taxa. Protoplasma *124*, 224–235.

Kollmann, R., and Glockmann, C. (1991). Studies on graft unions. III. on the mechanism of secondary formation of plasmodesmata at the graft interface. Protoplasma *126*, 19–29.

Kragler, F., Lucas, W.J., and Monzer, J. (1998). Plasmodesmata: dynamics, domains and patterning. Ann. Bot. *81*, 1–10.

Kuhn, C., Franceschi, V.R., Schultz, A., Lemoine, R., and Frommer, W.B. (1997). Macromolecular trafficking indicated by localization and turnover of sucrose transporters in enucleate sieve elements. Science *275*, 1298–1300.

Lucas, W.J. (1995). Plasmodesmata: intercellular channels for macromolecular transport in plants. Curr. Opin. Cell Biol. *7*, 673–680.

Lucas, W.J., Ding, B., and van der Schoot, C. (1993). Plasmodesmata and the supracellular nature of plants. New Phytol. *125*, 435–476.

Lucas, W.J., Bouche-Pillon, S., Jackson, D.P., Nguyen, L., Baker, L., Ding, B., and Hake, S. (1995). Selective trafficking of KNOTTED 1 homeodomain protein and its mRNA through plasmodesmata. Science *270*, 1980–1983.

Mezitt, L.A., and Lucas, W.J. (1996). Plasmodesmal cell-to-cell transport of proteins and nucleic acids. Plant Mol. Biol. *32*, 251–273.

Mizuhira, V., and Futaesaku, Y. (1971). On the new approach of tannic acid and digitonine to the biological fixatives. Proc. Electron Micros. Soc. Amer. *29*, 494–495.

Mizuhira, V., and Futaesaku, Y. (1972). New fixation for biological membranes using tannic acids. Acta Histochem. et Cytochem. *1*, 233–236.

Oparka, K.J., and Gates, P. (1981). Transport of assimilates in the developing caryopsis of rice (*Oryza sativa* L.). Ultrastructure of the pericarp vascular bundle and its connections with the aleurone layer. Planta *151*, 561–573.

Oparka, K.J., and Turgeon, R. (1999). Sieve elements and companion cells—traffic control centers of the phloem. Plant Cell *11*, 739–750.

Oparka, K.J., Boevink, P., and Santa Cruz, S. (1996). Studying the movement of plant viruses using green fluorescent protein. Trends Plant Sci. *1*, 412–418.

Oparka, K.J., Santa Cruz, S., Prior, D.A.M., Padgett, H.S., and Beachy, R.N. (1997). Gating of epidermal plasmodesmata is restricted to the leading edge of expanding infection sites of tobacco mosaic virus (TMV). Plant J. *12*, 781–789.

Overall, R.L., Wolfe, J., and Gunning, B.E.S. (1982). Intercellular communication in *Azolla* roots: I. ultrastructure of plasmodesmata. Protoplasma *111*, 134–150.

Palauqui, J.-C., Elmayan, T., Pollien, J.-M., and Vaucheret, H. (1997). Systemic acquired silencing: transgene-specific post-transcriptional silencing is transmitted by grafting from silenced stocks to non-silenced scions. EMBO J. *16*, 4738–4745.

Petty, I.T.D., and Jackson, A.O. (1990). Mutational analysis of barley stripe mosaic virus RNA. Virology *179*, 712–718.

Raven, J.A. (1997). Multiple origins of plasmodesmata. Eur. J. Phyco. *32*, 95–101.

Restrepo, M.A., Freed, D.D., and Carrington, J.C (1990). Nuclear transport of plant potyviral proteins. Plant Cell *2*, 1185–1194.

Roberts, A.G., Santa Cruz, S., Roberts, I.M., Prior, D.A.M., Turgeon, R., and Oparka, K.J. (1997). Phloem unloading in sink leaves of *Nicotiana benthamiana*: comparison of a fluorescent solute with a fluorescent virus. Plant Cell *9*, 1381–1396.

Ryabov, E.V., Oparka, K.J., Santa Cruz, S., Robinson, D.J., and Taliansky, M.E. (1997). Intracellular location of two groundnut rosette umbravirus proteins delivered by PVX and TMV vectors. Virology *242*, 303–313.

Sambrook, J., Fritsch, E.F., and Maniatis, T. (1989). Molecular Cloning: A Laboratory Manual, Second Edition (Cold Spring Harbor, NY: Cold Spring Harbor Laboratory Press).

Santa Cruz, S., Chapman, S., Roberts, A.G., Roberts, I.M., Prior, D.A.M., and Oparka, K.J. (1996). Assembly and movement of a plant virus carrying a green fluorescent protein overcoat. Proc. Natl. Acad. Sci. USA *93*, 6286–6290.

Santa Cruz, S., Roberts, A.G., Prior, D.A.M., Chapman, S., and Oparka, K.J. (1998). Cell-to-cell and phloem-mediated transport of potato virus X: the role of virions. Plant Cell *10*, 495–510.

Schulz, A. (1995). Plasmodesmal widening accompanies the short-term increase in symplasmic phloem unloading in pea roots under osmotic stress. Protoplasma *188*, 22–37.

Seagull, R.W. (1983). Differences in the frequency and disposition of plasmodesmata resulting from root cell elongation. Planta *159*, 497–504.

Siemering, K.R., Golbik, R., Sever, R., and Haseloff, J. (1996). Mutations that suppress the thermosensitivity of green fluorescenent protein. Curr. Biol. *6*, 1653–1663.

Simionescu, N., and Simionescu, M. (1976). Galloylglucoses of low molecular weight as mordant in electron microscopy. 1. procedure and evidence for mordanting effect. J. Cell Biol. *70*, 608–821.

Stiekema, W.J., Hiedekamp, F., Dirske, W.G., van Beckum, J., de Haan, P., ten Bosch, C., and Louwerse, J.D. (1988). Molecular cloning and analysis of four potato tuber mRNAs. Plant Mol. Biol. *11*, 255–269.

Terry, B.T., and Robards, A.W. (1987). Hydrodynamic radius alone governs the mobility of molecules through plasmodesmata. Planta *171*, 145–157.

Tilney, L.G., Cooke, T.J., Connely, P.S., and Tilney, M.S. (1990). The distribution of plasmodesmata and its relationship to morphogenesis in fern gametophytes. J. Cell Biol. *122*, 739–747.

Tomenius, K., Clapham, D., and Meshi, T. (1987). Localization by immunogold cytochemistry of the virus-encoded 30K protein in plasmodesmata of leaves infected with tobacco mosaic virus. Virology *160*, 363–371.

Tucker, E.B. (1982). Translocation in the staminal hairs of *Setcreasea purpurea*. I. study of cell ultrastructure and cell-to-cell passage of molecular probes. Protoplasma *113*, 193–201.

Tucker, E.B. (1993). Azide treatment enhances cell-to-cell diffusion in staminal hairs of *Setcreasea purpurea*. Protoplasma *174*, 45–49.

Turgeon, R. (1989). The sink–source transition in leaves. Annu. Rev. Plant. Physiol. Plant Mol. Biol. *40*, 119–138.

Voinnet, O., and Baulcombe, D.C. (1997). Systemic signaling in gene silencing. Nature *389*, 553.

Waigmann, E., Lucas, W.J., Citovsky, V., and Zambryski, P. (1994). Direct functional assay for tobacco mosaic virus cell-to-cell movement protein and identification of a domain involved in increasing plasmodesmal permeability. Proc. Natl. Acad. Sci. USA *91*, 1433–1437.

Wang, N., and Fisher, D.B. (1994). The use of fluorescent tracers to characterize the post-phloem transport pathway in maternal tissues of developing wheat grains. Plant Physiol. *104*, 17–27.

Wang, H.L., Offler, C.E., and Patrick., J.W. (1995). The cellular pathway of photosynthate transfer in the developing wheat grain. II. a structural analysis and histochemical studies of the pathway from the crease phoem to the endosperm cavity. Plant Cell Env. *18*, 373–388.

Wolf, S., Deom, C.M., Beachy, R., and Lucas, W.J. (1989). Movement protein of tobacco mosaic virus modifies plasmodesmal size exclusion limit. Science *246*, 377–379.

Wolf, S., Deom, C.M., Beachy, R.N., and Lucas, W.J. (1991). Plasmodesmatal function is probed using transgenic plants that express a virus movement protein. Plant Cell *3*, 593–604.

Wright, K.M., and Oparka, K.J. (1997). Metabolic inhibitors induce symplastic movement of solutes from the pathway phloem of *Arabidopsis* roots. J. Exp. Bot. *48*, 1807–1814.

Zhu, T., Lucas, W.J., and Rost, T.L. (1998). Directional cell-to-cell communication in the *Arabidopsis* root apical meristem. I. an ultrastructural and functional analysis. Protoplasma *203*, 35–47.